RADIATIVE DIVERTOR AND SOL EXPERIMENTS IN OPEN AND BAFFLED DIVERTORS ON DIII–D*

S.L. ALLEN,† N.H. BROOKS, R. BASTASZ,‡ J. BOEDO,Δ J.N. BROOKS,◊ J.W. CUTHBERTSON,Δ T.E. EVANS, M.E. FENSTERMACHER,† D.N. HILL,† D.L. HILLIS,# J. HOGAN,# R.C. ISLER,# G.L. JACKSON, T. JERNIGAN,# A.W. HYATT, C.J. LASNIER,† R. LEHMER,Δ A.W. LEONARD, M.A. MAHDAVI, R. MAINGI,# W.H. MEYER,† P.K. MIODUSZEWSKI,# R.A. MOYER,Δ D.G. NILSON,† L.W. OWEN,# T.W. PETRIE, G.D. PORTER,† M.E. RENSINK,† M.J. SCHAFFER, J. SMITH, G.M. STAEBLER, R.D. STAMBAUGH, D.M. THOMAS, M.R. WADE,# W.R. WAMPLER,‡ J.G. WATKINS,‡ W.P. WEST, D.G. WHYTE,Δ N. WOLF,† C.P.C WONG, R.D. WOOD,† AND THE DIII–D PHYSICS AND OPERATIONS TEAMS
DIII–D National Fusion Facility, General Atomics, San Diego, California 92186-5608

Abstract

We present recent progress towards an understanding of the physical processes in the divertor and scrape-off-layer (SOL) plasmas in DIII–D. This has been made possible by a combination of new diagnostics, improved computational models, and changes in divertor geometry. We have focused primarily on ELMing H-mode discharges. The physics of Partially Detached Divertor (PDD) plasmas, with divertor heat flux reduction by divertor radiation enhancement using D_2 puffing, has been studied in 2-D, and a model of the heat and particle transport has been developed that includes conduction, convection, ionization, recombination, and flows. Plasma and impurity particle flows have been measured with Mach probes and spectroscopy and these flows have been compared with the UEDGE model. The model now includes self-consistent calculations of carbon impurities. Impurity radiation has been increased in the divertor and SOL with "puff and pump" techniques using SOL D_2 puffing, divertor cryopumping, and argon puffing. The important physical processes in plasma-wall interactions have been examined with a DiMES probe, plasma characterization near the divertor plate, and the REDEP code. Experiments comparing single-null (SN) plasma operation in baffled and open divertors have demonstrated a change in the edge plasma profiles. These results are consistent with a reduction in the core ionization source calculated with UEDGE. Divertor particle control in ELMing H-mode with pumping and baffling has resulted in reduction in H-mode core densities to $n_{e\,/\,n_{gw}} \approx 0.25$. Divertor particle exhaust and heat flux has been studied as the plasma shape was varied from a lower SN, to a balanced double null (DN), and finally to an upper SN.

1. INTRODUCTION

We present in this paper progress towards an increased understanding of the relevant physical processes that are important in controlling: (a) the divertor heat flux with divertor and core radiation (Section 2), (b) impurity and deuteron concentrations with plasma flows and cryopumping (Section 3), and (c) erosion and redeposition at material walls in the divertor (Section 4). We have performed new experiments comparing operation with open and baffled divertors, and have demonstrated core density control in both low- and high-triangularity plasmas (Section 5). Core density control is an important tool for DIII–D where active profile control is planned with electron-cyclotron-current drive.

We have used new diagnostic measurements of key physics parameters in concert with state-of-the-art computational models (UEDGE-EIRENE-DEGAS, B2.5-EIRENE) to further our understanding of the fundamental physical processes. Shown in Fig. 1 is the DIII–D diagnostic set in the lower divertor, along with the quantities that are measured by each instrument. Recent improvements include: (a) 2-D measurements of carbon line and deuterium recombination radiation,

*Work supported by U.S. Department of Energy under Contracts DE-AC03-89ER51114, W-7405-ENG-48, DE-AC05-96OR22464, DE-AC04-94AL85000, and Grant No. DE-FG03-95ER54294.
†Lawrence Livermore National Laboratory, Livermore, California
‡Sandia National Laboratory, Livermore, California
ΔUniversity of California at San Diego, San Diego, California
◊Argonne National Laboratory, Argonne, Illinois
#Oak Ridge National Laboratory, Oak Ridge, Tennessee.

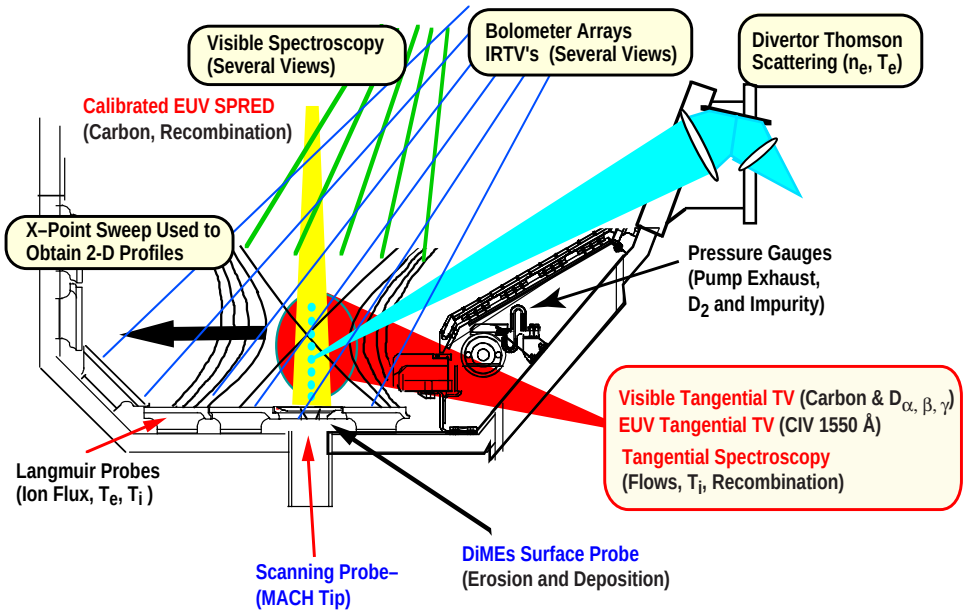

FIG. 1. The array of diagnostics (with quantity measured) in the lower divertor in DIII–D includes: Bolometer (48-channel, radiated power distribution), Scanning mach probe(deuterium flow), Infrared TV's (7-IRTV's-lower divertor heat flux at two toroidal locations, upper divertor, also inside wall), Tangential spectroscopy(neutral, impurity and deuteron flows, T_i, Recombination), Tangential TV (simultaneous inverted 2-D profiles of two lines: CII, CIII, D_α, D_β, D_γ, neutral density), DiMES surface probe (erosion and redeposition on carbon and tungsten samples), Target Langmuir probes (T_e, n_e, Γ_i-ion flux), EUV SPRED spectrograph with absolute intensity calibration(CIV, L_α, L_β, other impurity emissions), an EUV tangential camera (CIV 1550 Å 2-D images), Neutral pressure gauges (deuterium and impurity partial pressures in the edge plasma and pumping plenum), and an 8-channel divertor Thomson scattering system DTS (T_e, n_e the plasma is swept to obtain 2-D profiles).

including CIV (1550 Å), (b) measurement of plasma flows with spectroscopy and a Mach probe, and (c) erosion and redeposition measurements with a DiMES probe.

2. PHYSICS OF DIVERTOR HEAT FLUX REDUCTION

Starting from an empirical observation of the reduction of divertor peak heat flux with deuterium puffing [1], we have systematically measured the important terms in the heat and particle transport equations with new diagnostics; at present we have a 2-D characterization of much of the divertor region. Shown in Fig. 2(a) is a representative partially detached divertor (PDD) discharge [2], showing the reduction in peak heat flux, constant ELMing H–mode confinement, and controlled core density with cryopumping. Scaling experiments have shown that the outer strike point (OSP) peak heat flux can be reduced to nearly the same value, 1 MW m^{-2}, independent of input neutral beam power up to $P_{inj} \sim 14$ MW [3,4]. In Fig. 2(b) are plasma profiles at the OSP for a typical discharge set of attached and detached (dashed) discharges. The q_{div} (heat flux), Γ_i (ion flux), and P_e (electron pressure) are reduced at the OSP, but Γ_i increases outboard, hence the name partially detached divertor. The T_e from Divertor Thomson Scattering (DTS) is dramatically reduced to 1–2 eV, and this has been a key measurement in the interpretation of much of the divertor data.

A 2-D model of the PDD is shown in Fig. 2(c). To facilitate discussion of the changes of the parallel heat flow from an ELMing H–mode to PDD operation, we use a 1-D form of the parallel energy flow equation [5], where the first term is identified as the classical parallel heat conduction, the second term is convection, and $v_{//}$ is the parallel plasma fluid velocity. The losses S_E include radiation, ionization, and recombination:

$$\frac{d}{ds}\left\{\left(-\kappa T_e^{5/2}\frac{dT_e}{ds}\right)+nv_{\|}\left[\frac{5}{2}\left(T_i+T_e\right)+\frac{1}{2}m_i v_{\|}^2+I_o\right]\right\}=S_E \quad . \tag{1}$$

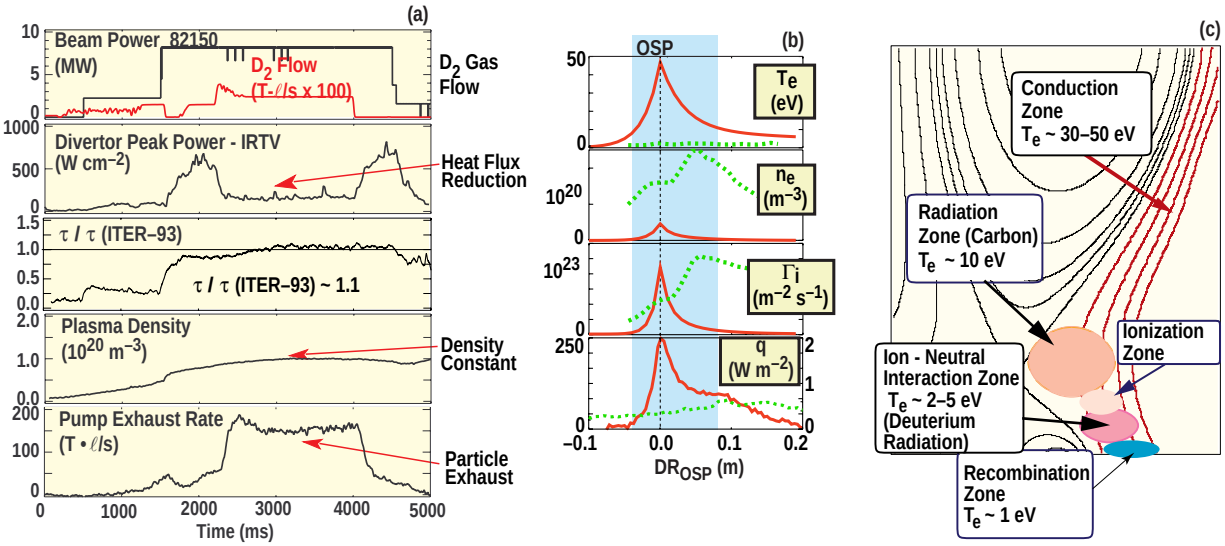

FIG. 2. (a) A representative PDD discharge (D_2 puffing) showing heat flux reduction, H–mode confinement, and controlled core density. (b) The T_e, n_e, Γ_i, and heat flux at the outer strike point for a representative attached and PDD (dashed) discharge. (c) The model that has been developed to explain the physical processes in the PDD discharge.

In the PDD, conduction carries the exhaust heat along the field line from the core to a region near the divertor. Here, carbon radiates strongly (10–12 eV), as indicated by calibrated EUV spectroscopy of the divertor region. Inversions of 2-D visible (CII, CIII) and ultraviolet (CIV 1550 Å) emissions indicate carbon radiates primarily near the X–point. The total radiation (mostly UV) from spectroscopy agrees well with corresponding chords of the bolometer. Ratios of calibrated multi-chord [6] and TV images in the visible ($Balmer_\alpha/B_\beta$) [7] indicate that recombination occurs near the divertor plate in the PDD as indicated in the model in Fig. 2(c) [8]. Corresponding ratios in the UV ($Lyman_\alpha/Ly_\beta$) show similar changes, but often suggest absorption of the Ly_α emission [9]. A radially-integrated form of Eq. (1) has shown that the measured T_e from DTS, the bolometer radiation, and q_{div} (from IRTVs) are consistent with conduction in ELMing H–mode, but convection is required in the PDD [10,11]. The implied radially-averaged $v_{//}$ is consistent with direct measurements of $M \sim 0.8$ in the divertor region [12] from the scanning Mach probe

The diagnostic set has enabled several other interesting observations: (a) there is a critical upstream separatrix density for PDD onset that scales roughly linearly with the input power [13]; (b) target Langmuir probe measurements indicate that electron kinetic effects are not important in ELMing H–mode or PDD plasmas [14], (c) the neutral density near the X–point has been measured to be $\sim 10^{17}$ m^{-3} in L–mode discharges from tangential TV views [15], and (d) the effect X–point geometry effects on boundary potentials and turbulence have been examined [16].

We have also performed "puff and pump" experiments with SOL deuterium puffing (up to 2.5×10^{22} D^0 s^{-1}), exhaust with cryopumping, and impurity injection. In trace injection experiments, exhaust enrichment up to 17 was obtained with argon, and enhanced radiation in the divertor and SOL has also been obtained with argon [17]. For the conditions on DIII–D, we find that the argon and carbon radiation in the divertor increase by equal amounts, but models [18] indicate that this need not be the case in future machines operating in different temperature regimes.

We explored the source of carbon by comparing L–mode helium with L–mode deuterium plasmas, and the dramatic decrease in the carbon radiation suggests that chemical sputtering plays a role in the source. However, the total divertor radiation in these discharges was unchanged because the carbon radiation was replaced by helium radiation. Modeling with the MCI Monte-Carlo code suggests that standard chemical sputtering models overestimate the amount of carbon we measure experimentally [19].

3. PLASMA AND IMPURITY FLOWS AND COMPARISON WITH MODELS

We have studied plasma flows both to further our understanding of the convective heat flow discussed above and to understand impurity transport in the divertor and SOL. Active control of impurities, like enrichment achieved with "puff and pump" techniques discussed above, is an approach to increase the operational window of radiative divertor plasmas and a method to control

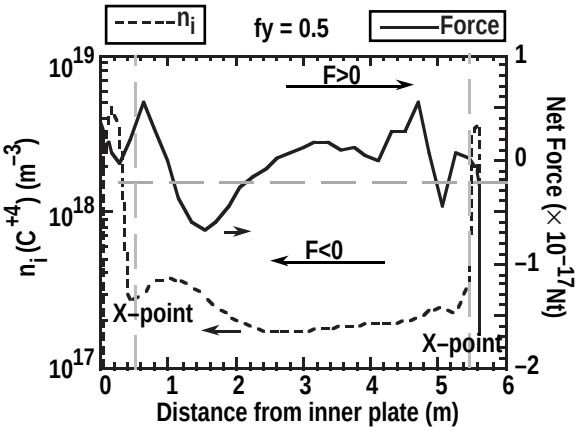

FIG. 3. The ion density and net force on C4⁺ ions (right) from UEDGE, the gradient in the force near a force null (e.g. near 0.4 and 1 m) determines whether the ion density builds up or is depleted.

core impurity content. We have made recent improvements to the UEDGE code, including realistic models of chemical and physical sputtering [20], to model impurity transport for comparison with data. The UEDGE code has been benchmarked with a variety of DIII–D discharges [21], and it calculates multi-species impurity transport. In Fig. 3 are the poloidal distributions of the C4⁺ ion density (the charge state flowing into the core) and net parallel particle force. Impurity accumulation or depletion is determined by the force gradient near a force null, and the position of this null is determined by the details of the parallel ion temperature gradient and the flow pattern of the fuel ion species (i.e. the frictional drag term).

One strength of the UEDGE modeling is the ability to calculate predicted diagnostic data directly (e.g., the Mach probe does not scan along a field line). In Fig. 4(a), we compare direct measurements of the deuteron Mach number from a scanning probe [12,22] with a UEDGE calculation of the data. The data were obtained along a vertical cut through the plasma in the SOL, and the UEDGE results were calculated for the same discharge and plasma shape. The flow in the SOL is towards the plate. In Fig. 4(b) is a comparison of the C⁺ ion velocity distribution [6,23] from a tangential spectrometer chord and the UEDGE calculation. There is usually a flow away from the plate near the separatrix, and a flow towards the plate farther out in the SOL. As shown in Fig. 4, there is reasonable agreement between the data and the model in attached discharges. In detached discharges, at the location of the Mach probe, we do not see a large change in the flow velocity, but the 2-D UEDGE calculation indicates that there are strong gradients and more 2-D data is required for a better comparison. The measured carbon velocities tend to be more towards the plate in detached discharges: the flow away from the plate decreases, and the flow towards the plate increases. Detailed comparisons with multiple chords of spectroscopy are in progress.

We have also identified new, interesting physics in the interface between the SOL and the "private flux" region below the x-point. A reversal in the plasma parallel flow has been observed by

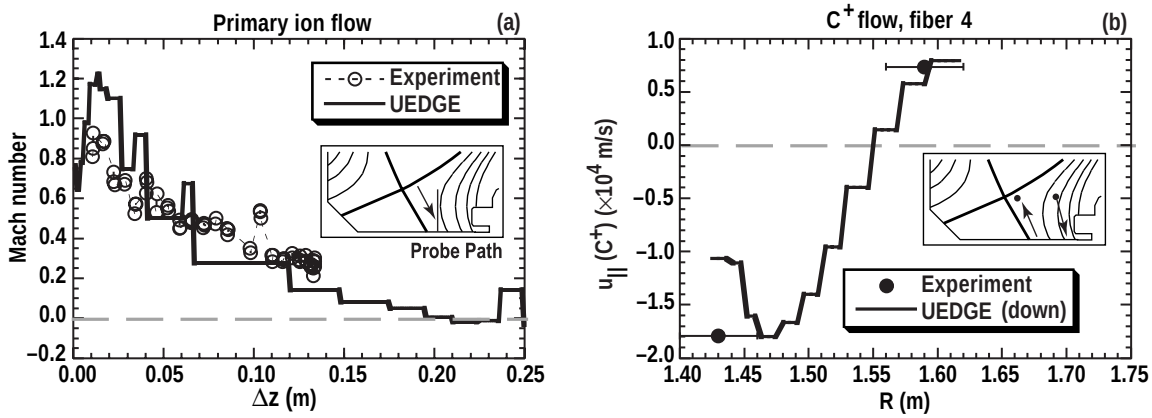

FIG. 4. Comparisons of measurements of (a) primary ion flow from the Mach probe and (b)C+ velocity from spectroscopy with calculations from the UEDGE code for an (OSP-attached) ELMing H–mode.

the Mach probe, as shown in Fig. 5(a). Potential measurements from the probe also indicate large radial electric fields. The corresponding E×B drifts can drive an appreciable fraction of the recycling flux from the outer leg poloidally across the private region to the inner leg. The DTS system also measures large plasma density in the private flux region. We have also observed significant recombination radiation in the private flux region during the transition to outer leg detachment. The UEDGE model can now include drifts in the calculation, and comparisons with data are in progress [24].

4. EROSION AND REDEPOSITON MEASUREMENTS AND MODELING

To predict the lifetime of plasma-wall surfaces in future machines, we must understand the physical processes taking place between the divertor plasma and the target plate material. We have made direct measurements of erosion and redeposition at the OSP with an insertable DiMES probe [25] for comparison with models. A key to the comparison of these data with experimental models is the characterization of the plasma near the probe with the diagnostics shown in Fig. 1 and the data in Fig. 2(b), as the determination of quantities such as the input ion flux, prompt redeposition, and self-sputtering require these data. Shown in Fig. 6 is a comparison of the gross and net erosion obtained from a carbon DiMES sample in an attached plasma, along with a calculation from the REDEP code [26]. Also shown (right) are the erosion for attached (solid) and PDD (dashed) plasma operation for carbon and tungsten DiMES samples. Note the dramatically reduced erosion near the strike point in the carbon sample for the PDD case. The erosion rates for the attached cases are greater than 10 cm/exposure-year, even with incident heat flux <1 MW/m^2. In this case, measurements and modeling agree for both gross and net carbon erosion, showing the near- surface transport and redeposition of the carbon is well understood. Self-sputtering and oblique incidence are important, and the effective sputtering yields exceed 10%. The private flux wall is measured to be a region of net redeposition with attached divertor plasmas. Divertor plasma detachment eliminates physical sputtering, spectroscopically measured chemical erosion yields are also found to be low (Y(C/D$^+$) ≤ 10^{-3}). This leads to suppression of net erosion at the outer strike-point, which becomes a region of net redeposition (~4 cm/exposure-year). Leading edge erosion, and subsequent carbon redeposition, caused by tile gaps can account for half of the deuterium codeposition in the DIII–D divertor.

5. PARTICLE CONTROL WITH BAFFLING AND CRYOPUMPING

We have recently installed and conditioned a new upper divertor baffle and cryopump whose geometry is matched for particle control in high-δ plasmas (δ ~ 0.7). The shape of the baffle was designed with a combination of UEDGE and DEGAS modeling [27], and the width is a optimum

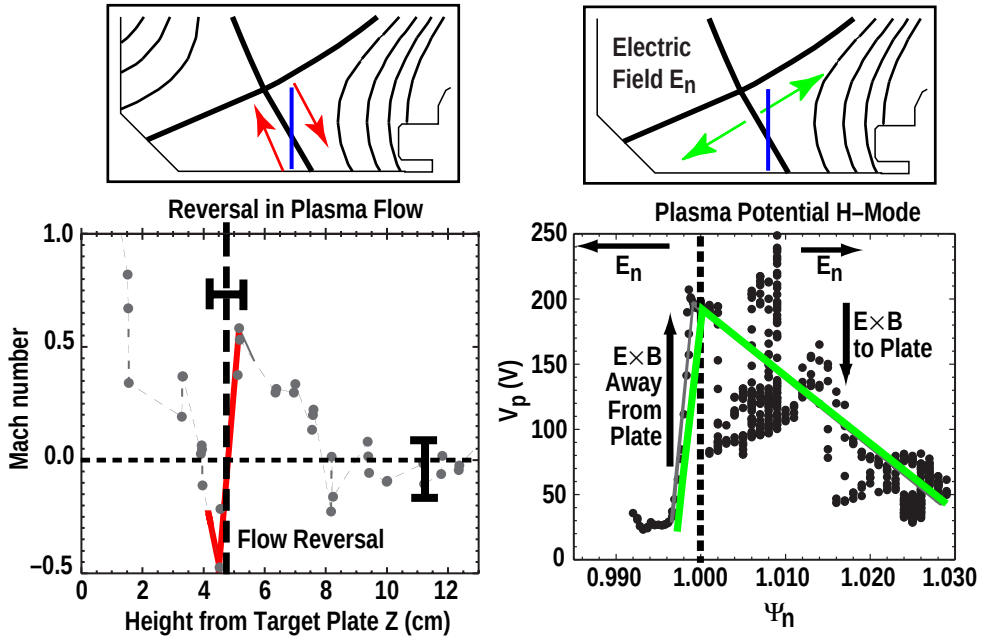

FIG. 5. We are observing new physics at the separatrix between the outer SOL and the private flux region. There is a reversal in the main ion flow (left) and a sharp change in the potential (right), implying an electric field. The corresponding ExB drifts can drive appreciable particle currents.

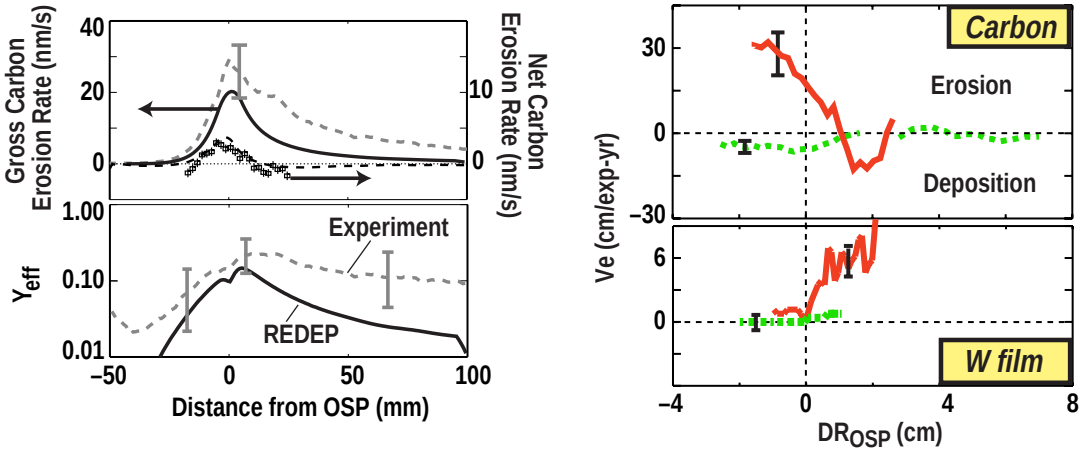

FIG. 6. (Left) The gross and net erosion from the DiMES probe (dashed) compared with the REDEP code (solid) in attached plasma operation. The effective sputtering yield agrees well with the code prediction. (Right) The effective sputtering yield for carbon (top) and tungsten (bottom) for attached (solid) and detached (dashed) plasma operation; note the reduction in erosion for the PDD case.

between a very closed baffle for neutrals (which can introduce recycling directly into the plasma core), and a open baffle that allows neutral leakage (with little recycling). A detailed comparison of unpumped open/closed divertor operation was carried out with carefully matched plasmas as shown in Fig. 7; the ion ∇B drift was towards the plate in each case. We observed that the line-average density was very similar in the two cases, but the midplane H_α (a tangential view just inside the separatrix) was reduced for the closed case. The density gradient at the separatrix, a measure of the core ionization rate, is reduced in the closed geometry. Transport modeling indicates that the ratio of the (open/closed) core ionization source was reduced by a factor of about F = 2.6; we normalized to the target plate current for each discharge. No changes in energy confinement during ELMing H–mode operation were observed, but the density at which the PDD occurred was decreased by 20% in the closed divertor.

We compared the measured reduction in core ionization with two computational models. A UEDGE model, in which the density profile is self-consistently calculated with a fluid neutrals model results in an estimate of F = 2. We have also calculated F = 3.8 for a fixed UEDGE core plasma model and a full Monte-Carlo neutrals calculation with DEGAS [27,28]. Coupled self-consistent

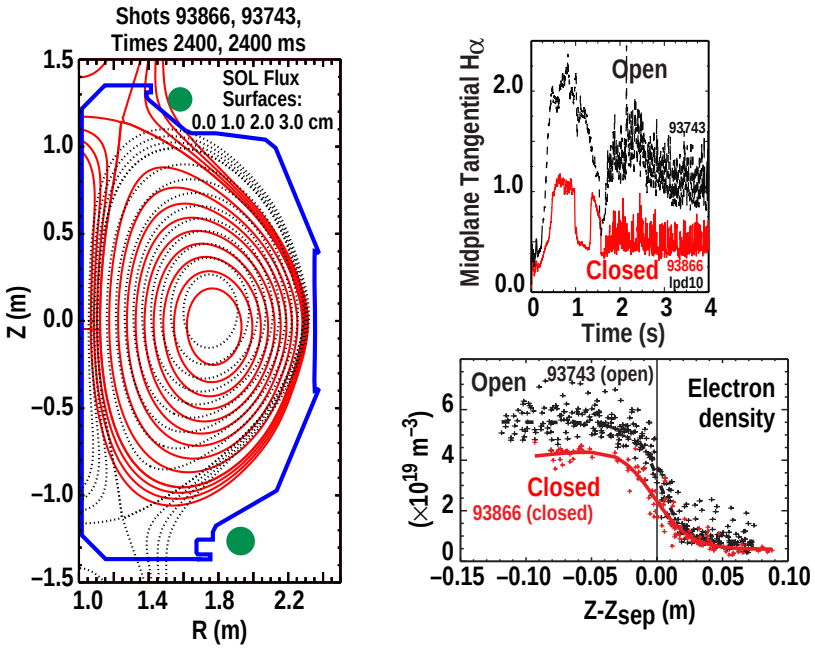

FIG. 7. Carefully matched plasmas were used for comparison of open (dashed) and baffled (solid) divertor configurations. We observed a drop in the edge tangential H_α signal, and a change in the edge density profile, implying a net reduction in the core ionization source with the baffled divertor.

UEDGE-EIRENE calculations are in progress. Using the second technique, we estimate for a more closed divertor with a private-flux space "dome" and inside baffle that F = 9 for SN operation. A full double null installation is required for F = 9 for DN. The UEDGE modeling has also shown that the shape of the baffle can influence the plasma flows, and we are optimizing the shape to see if more effective enrichment of impurities is possible in a closed divertor.

With the upper cryopump on, we achieved active density control with $n_e/n_{GW} = 0.27$ (fraction of the Greenwald density), which is close to the 0.22 achieved with the lower pump. This establishes an important particle control tool for high-δ plasma operation in DIII–D. The particle exhaust of the upper pump is similar to the lower pump, except at low $n_e < 5\times10^{19}$ m^{-3}. We are currently determining if this low exhaust at low density is due to better wall conditioning or reduced pumping effectiveness. Wall conditioning has controlled impurities in the baffled divertor so that $Z_{eff} \sim 2$. We routinely injected trace neon impurities to measure the core impurity confinement in several configurations. We found that at high density, the core neon decay time was similar for upper and lower divertors, but at low density, the time was significantly longer for the upper baffled pump.

6. DOUBLE NULL DIVERTOR PLASMA OPERATION

We have continued research in double null divertor plasma operation. Previously, we showed that a balanced up/down heat flux required an unbalanced magnetic configuration [4]. Recent density control experiments with the upper high-δ cryopump have shown that the pump exhaust (with one pump in a balanced DN configuration) is about 50% of that in a single null plasma. As shown in Fig. 8, a nearly upper single-null plasma (with drsep = 5 cm, the distance between the two separatrices mapped to the midplane) is required to obtain maximum exhaust with one pump.

We have also observed that the role of neutrals may be different between DN and SN discharges [29], in that D_2 gas puffing in DN discharges produced only modest reductions in P_e, and core MARFEs were not observed, even at n_e approaching n_{GW}.

7. CONCLUSIONS AND FUTURE WORK

In conclusion, we have used a comprehensive diagnostic set and state-of-the art computational models to gain a better understanding of convective heat flow, recombination processes, deuteron and impurity ion flows, and the effect of divertor geometry and baffles. In 1999, we will install a third divertor cryopump, private-flux-space dome, and inside baffle which will is expected to provide particle control at the inner strike point and increase our particle control capability in high-δ plasmas. New diagnostics, such as a Penning gauge and spectroscopy chords in the upper divertor, will be added to study the impurity effects in the more baffled divertor.

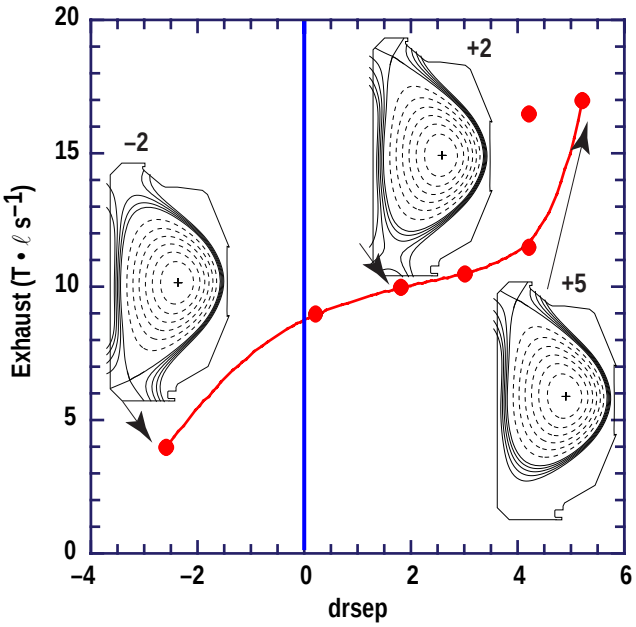

FIG. 8. The pump exhaust to the upper cryopump as a function of SN and DN plasmas. The abscissa, drsep, is the distance between the upper and lower separatrix measured at the midplane, drsep = 0 is a magnetically balanced double null plasma.

REFERENCES

[1] HILL, D.N., et al., Proc. 15th Int. Conf. on Plasma Phys. and Contr. Nucl. Fusion Research, Seville, Spain (International Atomic Energy Agency, Vienna, 1995) Paper IAEA-CN-60/A4-2, p. 499.
[2] PETRIE, T.W., et al., Nucl. Fusion **37**, 321 (1997).
[3] LASNIER, C.J., et al., "*Scaling and Profiles of Heat Flux During PDD in DIII–D,"* Proc. of the 13th Inter. Conf. on Plasma Surface Interactions in Contr. Fusion Devices, San Diego, California, 1998, to be published.
[4] LASNIER, C.J., HILL, D.N., et al., Nucl. Fusion **38**, 1225 (1998).
[5] BRAGINSKII, S.I., *Reviews of Plasma Physics* (Consultants Bureau, New York, 1965).
[6] ISLER, R.C., et al., "*Spectroscopic Measurements of Ion Temperatures and Parallel Flows in the DIII–D Tokamak,*" Proc. of the 13th Inter. Conf. on Plasma Surface Interactions in Contr. Fusion Devices, San Diego, California, 1998, to be published.
[7] FENSTERMACHER, M.E., et al., *Physics of the Detached Radiative Divertor Regime in DIII–D,* Proc. of the 25th EPS Conf. on Contr. Fusion and Plasma Phys., Prague, Czech Republic, 1998, to be published.
[8] FENSTERMACHER, M.E., et al., Phys. Plasmas **4**, 1761 (1997).
[9] WOOD, R.D., et al., Bull. Am. Phys. Soc. **42**, 1844 (1998).
[10] LEONARD, A.W., et al., Phys. Rev. Lett. **78**, 4769 (1997).
[11] LEONARD, A.W., et al., Phys. Plasmas **5**, 1736 (1998).
[12] BOEDO, J., et al., "*Plasma Flow in the DIII–D Divertor,"* Proc. of the 25th EPS Conf. on Contr. Fusion and Plasma Phys., Prague, Czech Republic, 1998, to be published.
[13] MAINGI, R., et al., "*Density Limit Studies on DIII–D,*" Proc. of the 13th Inter. Conf. on Plasma Surface Interactions in Contr. Fusion Devices, San Diego, California, 1998, to be published.
[14] WATKINS, J.G., et al., "*Kinetic Effects,*" Proc. of the 13th Inter. Conf. on Plasma Surface Interactions in Contr. Fusion Devices, San Diego, California, 1998, to be published.
[15] COLCHIN, R.J., et al., "*Method of Neutral Density Determination Near the X-Point in DIII–D,*" Proc. of the 25th EPS Conf. on Contr. Fusion and Plasma Phys., Prague, Czech Republic, 1998, to be published.
[16] MOYER, R.A., et al., "*Potentials, ExB Drifts, and Fluctuations in Attached and Detached Divertors,"* Proc. of the 13th Inter. Conf. on Plasma Surface Interactions in Contr. Fusion Devices, San Diego, California, 1998, to be published.
[17] WADE, M.R., et al., "*Impurity Enrichment and Radiative Enhancement Using Induced SOL Flow in DIII–D," Proc.* of the 13th Inter. Conf. on Plasma Surface Interactions in Contr. Fusion Devices, San Diego, California, 1998, to be published.
[18] WADE, M.R., et al., "*Impurity Control Studies Using SOL Flow in DIII-D,"* these Proceedings.
[19] EVANS, T.E., et al., "*Qualitative Comparisons Between Experimenally Measured 2-D Carbon Radiation and MCI Code Simulations,*" Proc. of the 13th Inter. Conf. on Plasma Surface Interactions in Contr. Fusion Devices, San Diego, California, 1998, to be published.
[20] DAVIS, J.W., HAAS, A.A., J. Nucl. Mater. **241-243**, 37-51 (1997).
[21] PORTER, G.D., ALLEN, S.L., BROWN, M., et al., Phys. Plasmas **3**, 1967 (1997).
[22] BOEDO, J.A., et al., "*Flow Reversal, Convection, and Modeling in the DIII–D Divertor,*" submitted to Phys. Plasmas.
[23] ISLER, R.C., et al., submitted to Phys. Plasmas (1998).
[24] ROGNLIEN, T.D., et al., "*Influence of ExB and Grad-BTerms in 2-D Edge/Sol Transport Simulations,* " Proc. of the 13th Inter. Conf. on Plasma Surface Interactions in Contr. Fusion Devices, San Diego, California, 1998, to be published.
[25] WONG, C.P.C., et al., J. Nucl. Mater. **241-243**, 871 (1992).
[26} BROOKS, J.N., et al., Phy. Fluids B (Plasma Physics) **2**, 1858 (1990).
[27] FENSTERMACHER, M.E., J. Nucl. Mater. **220**, 330 (1995).
[28] ALLEN, S.L., et al., "*Studies of Baffled and Open Pumped Divertor Operation on DIII–D,*" Proc. of the 13th Inter. Conf. on Plasma Surface Interactions in Contr. Fusion Devices, San Diego, California, 1998, to be published.
[29] PETRIE, T.W., et al., "*The Role of Neutrals in the H-L Back Transition of High-Density SN and DN Gas Fueled Discharges on DIII–D,*" Proc. of the 13th Inter. Conf. on Plasma Surface Interactions in Contr. Fusion Devices, San Diego, California, 1998, to be published.